Nucleophilic Attack upon Ethylene co-ordinated to Mercury(II): A Molecular-orbital Study concerning the Origin of the Acceleration by Hg^{II} †

Shigeyoshi Sakaki,* Katsuhiko Maruta, and Katsutoshi Ohkubo
Department of Synthetic Chemistry, Faculty of Engineering, Kumamoto University, Kurokami, Kumamoto 860, Japan

An *ab initio* molecular-orbital study has been carried out on the nucleophilic attack upon free C_2H_4, $[Li(C_2H_4)]^+$, and $[HgH(C_2H_4)]^+$. It is clearly shown that the nucleophilic attack is difficult in the first two systems but very easy in $[HgH(C_2H_4)]^+$. An important factor in the metal-accelerated nucleophilic attack is the energy level of the metal acceptor orbital; because the acceptor orbital of HgH^+ lies low in energy, the exchange repulsion between the nucleophile and the olefin decreases and the bonding interaction between the nucleophile and olefin increases, leading to the acceleration. Changes in geometry and electron distribution caused by the nucleophilic attack have been investigated in detail and are explained on the basis of orbital mixing.

It is well known that although nucleophilic attack towards a free olefin is very difficult a nucleophile can easily react with an olefin complexed with Hg^{II}, Pd^{II}, and in several transition-metal complexes.[1] Such metal-accelerated nucleophilic attack is included as a key step in many catalytic reactions of transition-metal complexes. It is interesting and worthwhile to examine why the reactivity of olefins towards nucleophiles is increased by co-ordination to metals, and this has been investigated in several theoretical works.[2] Recently, Eisenstein and Hoffmann[3] proposed an elegant explanation of why the olefin is activated, in which the unsymmetrical complexation of the olefin was regarded as important. However, there was no indication why this was a necessary condition for a symmetrical olefin. Further, it has not been reported how the electronic structure and geometry of a metal–olefin complex change upon nucleophilic attack to form the final product and why non-transition metals do not accelerate this attack, excepting a few cases such as Tl^{3+} and Pb^{4+}.

In this work, an *ab initio* molecular-orbital (m.o.) study has been carried out on the nucleophilic attack towards free ethylene, ethylene complexed with Li^+, and ethylene complexed with Hg^{II}. The mercury(II)–ethylene complex was chosen because co-ordination of olefins to Hg^{II} greatly accelerates the nucleophilic attack and such attack is considered an important step in oxymercuration.[1,4] The other two systems were investigated for comparison. We have attempted to clarify why the nucleophilic attack is accelerated by co-ordination to Hg^{II}, but only little by co-ordination to Li^+, and what factors are important in the acceleration. It is also our intention to elucidate the changes in electronic structure and geometry found in this reaction system.

M.o. Calculation and Geometries

The *ab initio* m.o. calculations were carried out by using the IMSPAK program.[5] For the Hg atom, the relativistic effective core potential, proposed by Basch and Topiol,[6] was employed with a valence set [2*s* 2*p* 2*d*] contracted from (3*s* 3*p* 4*d*) primitives.‡ For ligand atoms, the usual 3-21G basis set[7] was used in the geometry optimization. In more detailed calculations, the 3-21 + G basis set[8] was employed only for the C atom, to take account of the negative charge accumulated on the C atom by the nucleophilic attack. In the present calculations, only a closed-shell singlet state was examined, because both the Li^+ and Hg^{2+} reaction systems have very stable closed-shell singlet states as the ground state and the nucleophilic attack is not considered to cause homolytic bond fission. The electronic structures of these reaction systems are expected to be described well by the usual closed-shell Hartree-Fock Roothaan LCAO-SCF m.o. method.

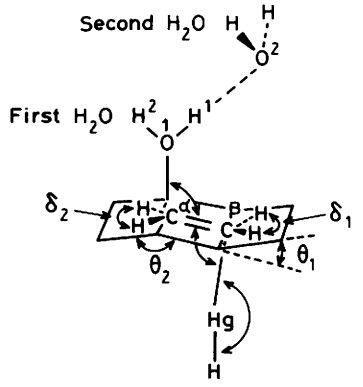

Figure 1. Co-ordinate system for $[HgH(C_2H_4)]^+ \leftarrow OH_2 \cdots OH_2$. Similar co-ordinate systems were taken for the other reaction systems such as $C_2H_4 \leftarrow OH_2 \cdots OH_2$ and $[Li(C_2H_4)]^+ \leftarrow OH_2 \cdots OH_2$

The ions $[Li(C_2H_4)]^+$ and $[HgH(C_2H_4)]^+$ were employed as models of the Li^+–olefin and Hg^{II}-olefin complexes.§ The geometries of these complexes were optimized by using the gradient technique.[9,10] The optimized geometrical parameters are as follows: in $[Li(C_2H_4)]^+$, Li–C 2.45, C=C 1.33 Å, CH_2 back bending 6°; in $[HgH(C_2H_4)]^+$, Hg–C 2.54, C=C 1.35 Å,

† *Non-S.I. units employed:* eV ≈ 1.60 × 10^{-19} J, cal = 4.184 J.

‡ The effective core potential with these basis sets gives optimized bond distances in agreement with experimental values: Hg–H in $[HgH]^+$, 1.58 Å (obs. 1.59 Å; G. Herzberg, 'Molecular Spectra and Molecular Structure,' Van Nostrand Reinhold, Cincinnati, 1950, vol. 1, p. 538); Hg–C in $Hg(CH_3)_2$, 2.08 Å (obs. 2.083 Å; K. Kashiwabara, K. Konaka, T. Iijima, and M. Kimura, *Bull. Chem. Soc. Jpn.*, 1973, **46**, 407).

§ The active species in oxymercuration has not been isolated, but is considered to include the olefin and one anionic ligand. Further, the presence of $[Hg(CH_3)(C_2H_4)]^+$ has been proposed in ion cyclotron resonance (R. D. Back, J. Patane, and L. Kevan, *J. Org. Chem.*, 1975, **40**, 257; R. G. Back, A. T. Weibel, J. Patane, and L. Kevan, *J. Am. Chem. Soc.*, 1976, **98**, 6237). It is not certain whether $[HgH(C_2H_4)]^+$ is a good model for oxymercuration, but this complex is similar to $[Hg(CH_3)(C_2H_4)]^+$ and seems to be realistic enough to compare the reactivity of the Hg^{II}–ethylene complex with that of $[Li(C_2H_4)]^+$ and free C_2H_4.

CH_2 back bending 7°, HgH 1.57 Å {Hg–C 2.56 and 2.57 Å in $[Hg(C_6Me_6)(CF_3CO_2)]_2$[11]}. In the investigation of nucleophilic attack, a water molecule was employed as a model of the nucleophile ROH and it was placed on the opposite side of Li^+ and Hg^{2+}, as shown in Figure 1, because oxymercuration proceeds with *trans* attack of the nucleophile.[1,4] The geometries of the reaction systems were optimized by a single parabolic fitting of the total energies, in which the distance between the O^1 and C^α atoms was taken as a reaction co-ordinate (see Figure 1). The following parameters were optimized: distances, Hg–H(hydride), Hg–C^β, C^α–C^β, O^1–H^1, and O^1–H^2; angles, $C^\alpha C^\beta Hg$, $C^\beta HgH$, $OC^\alpha C^\beta$, $HC^\alpha H$, $HC^\beta H$; and back bendings, $C^\alpha H_2$ and $C^\beta H_2$.

The second water molecule was added near to the first, because the H atom of the latter becomes protonic upon nucleophilic attack and probably forms a hydrogen bond with the surrounding solvent to stabilize itself.* The O^1–H^1 and O^2–H^1 distances were optimized, keeping fixed the geometries of the second water and the other part of $[M(C_2H_4)]^+ \leftarrow OH_2$ (see Figure 1 for O^1–H^1 and O^2–H^1).

The energy-decomposition analysis of Kitaura and Morokuma[12] was applied to this reaction system in order to examine which type of interaction between $[M(C_2H_4)]^+$ and H_2O is important. In this method, the binding energy (BE) is defined as in equation (1) where op indicates optimized; DEF is the deformation energy which is defined [equation (2)] as the

$$BE = E_t[M(C_2H_4)\leftarrow OH_2] - E_t[M(C_2H_4)]_{op} - E_t(OH_2)_{op} = INT + DEF \quad (1)$$

$$DEF = E_t[M(C_2H_4)]_{dis} - E_t[M(C_2H_4)]_{op} + E_t(H_2O)_{dis} - E_t(H_2O)_{op} \quad (2)$$

destabilization energy required to distort each fragment from its optimized structure to the deformed one taken over the total reaction system $[M(C_2H_4)\leftarrow OH_2]$. The interaction energy, INT, is defined as the stabilization with respect to the fragments

$$INT = E_t[M(C_2H_4)\leftarrow OH_2] - E_t[M(C_2H_4)]_{dis} - E_t(H_2O)_{dis} = ES + EX + FCTPLX + BCTPLX + R \quad (3)$$

calculation of the mercury reaction system, ES and EX cannot be separated from each other because the effective core potential used for the core orbitals of Hg includes a repulsive operator for electrons belonging to different nuclei. The static energy (ESX) is used in a discussion of such a case, and corresponds to the sum of ES and EX calculated for all the electrons. It is noted here that FCTPLX is not divided into two such terms as the charge transfer from H_2O to $M(C_2H_4)$ and the polarization term of $M(C_2H_4)$. Although this would be possible, the charge transfer is strongly coupled with the polarization as will be described later, and therefore further sub-division is not meaningful. Sub-division of BCTPLX is also not carried out.

Results and Discussion

Total Energies and Geometries.—The total energy change is shown in Figure 2, where (I) and (II) indicate the use of the 3-21 + G and 3-21G bases for the C atom, and lines (*a*) and (*b*) represent the energy changes with and without the second water molecule, respectively. The use of 3-21 + G gives a total energy change similar to that with 3-21G, probably because the net negative charge accumulated on the C atom is not as large as on a carbanion which would need the 3-21 + G basis set. Thus, the diffuse *sp* Gaussian function supplemented in the 3-21 + G basis set is of little importance in the m.o. study of nucleophilic attack.

The energy changes caused by the approach of the water molecule are significantly different in the three reaction systems. Apparently, it is very difficult for H_2O to approach free C_2H_4, and the total energy change is influenced little by the second H_2O. The attack of H_2O on $[Li(C_2H_4)]^+$ causes energy stabilization to some extent when the distance $R_{C^\alpha-O}$ = 2.5—3 Å. This stabilization seems to correspond with the solvation,

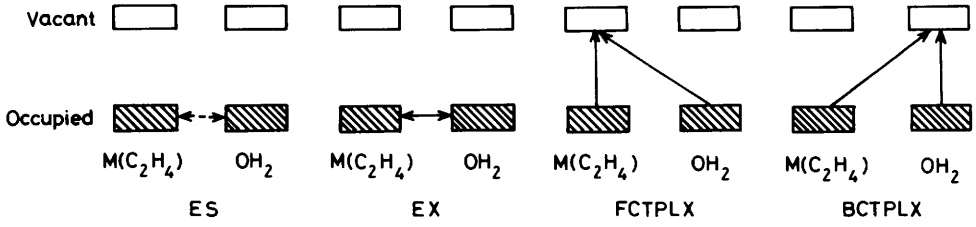

Scheme 1.

in their distorted structures. It is divided into several chemically meaningful terms, such as electrostatic (ES), exchange repulsion (EX), forward charge transfer and polarization of $M(C_2H_4)$ (FCTPLX), back charge transfer and polarization of H_2O (BCTPLX), and the higher-order coupling term (R) [equation (3)]. They are represented schematically in Scheme 1. In the m.o. because the geometry of $[Li(C_2H_4)]^+$ is little changed by the approach of H_2O to within 2.5—3 Å. Closer approach of H_2O, however, results in destabilization, by increasing the total energy. This suggests that although H_2O can approach $[Li(C_2H_4)]^+$ to within solvation distances it cannot approach the C_2H_4 ligand as close as the C–O covalent bond distance (*i.e.* $R_{C^\alpha-O}$ *ca.* 1.5 Å). In the case of $[HgH(C_2H_4)]^+$, H_2O can approach the C_2H_4 part as close as $R_{C^\alpha-O}$ = 1.6 Å with little barrier, when the second water molecule is absent. In the presence of the second H_2O, the total energy becomes stable at $R_{C^\alpha-O}$ = 1.5 Å, which corresponds to the formation of the C–O covalent bond. Thus, it can be concluded that nucleophilic attack on C_2H_4 cannot be accelerated by Li^+, but is very greatly accelerated by Hg^{II}.

Optimized structures are shown in Figure 3. According to expectation, the C^α–C^β and O^1–H^1 bonds are lengthened, $C^\alpha H_2$ and $C^\beta H_2$ bendings result, and the $MC^\alpha C^\beta$ angle (M = Li or Hg) is opened by the approach of H_2O. All of these

* The hydrogen-bonding interaction between the first and the second water molecules significantly influences the total energy change upon nucleophilic attack (Figure 2), which means that this hydrogen bond must be taken into consideration when considering information about the energy change. Solvation of the metal is also important. However, its strength seems to change during the nucleophilic attack to a lesser extent than that of the above-mentioned hydrogen bond, because changes in electron density and the Mulliken population of the water region are larger than those of the metal region (Figures 5 and 6). It is not easy to include both hydrogen bonding and solvation, and therefore only the former was examined here.

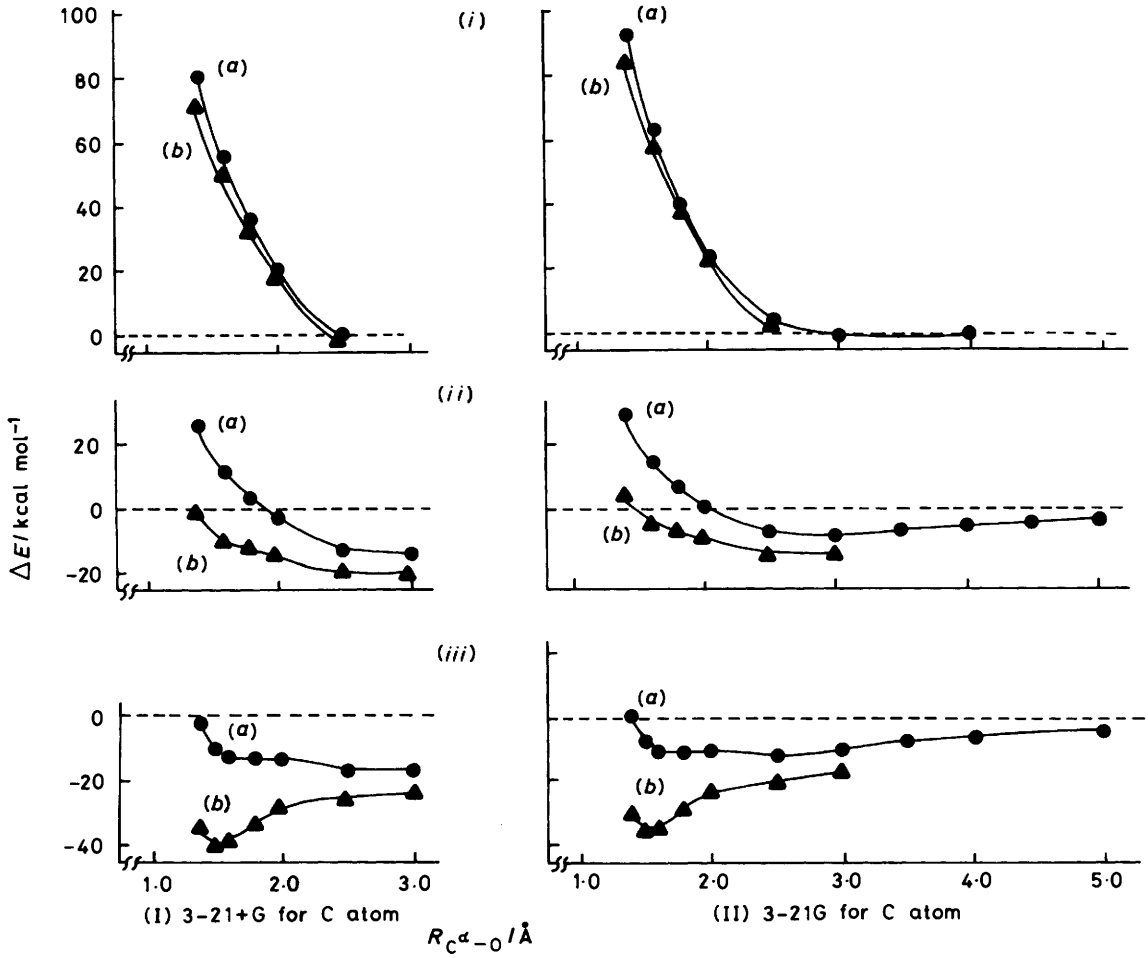

Figure 2. Total energy change caused by the approach of H_2O. Lines (*a*) and (*b*) represent the absence and the presence of the second water molecule, respectively. Systems: (*i*) C_2H_4←OH_2; (*ii*) $[Li(C_2H_4)]^+$←OH_2; and (*iii*) $[HgH(C_2H_4)]^+$←OH_2

transformations correspond to a gradual change in the C=C double bond to a single bond. Though similar changes arise in the three reaction systems, the geometry of $[HgH(C_2H_4)]^+$←OH_2 is closest to that of the final product. In other words, the system which is highly reactive towards nucleophilic attack facilitates formation of the final product.

Energy Decomposition Analysis (e.d.a.) between $M(C_2H_4)$ *and* H_2O.—E.d.a. was carried out at a rather early stage of the reaction (C^α–O 2.5—1.8 Å), because it is effective when the wavefunction of $M(C_2H_4)$←OH_2 can be approximated by a product of perturbed wavefunctions for the isolated $M(C_2H_4)$ and H_2O. As shown in Figure 4(*a*)—(*c*), the static interaction, ESX, becomes unstable with approach of H_2O, because the increase in the EX destabilization exceeds that of the ES stabilization.* Of the covalent interactions, only the FCTPLX interaction becomes strong with approach of H_2O and stabilizes the reaction system, whereas BCTPLX and R change little. The differences in ESX and FCTPLX among these reaction systems are compared in Figure 4(*d*) and (*e*), where solid lines indicate the difference $E[HgH(C_2H_4)^+$←$OH_2]$ – $E(C_2H_4$←$OH_2)$ and dashed lines the difference $E[Li(C_2H_4)^+$←$OH_2]$ – $E(C_2H_4$←$OH_2)$. Apparently, the most reactive $[HgH(C_2H_4)]^+$ system suffers the smallest destabilization of the ESX interaction and receives the largest stabilization of the FCTPLX interaction. The $[Li(C_2H_4)]^+$ system suffers a smaller ESX destabilization and receives a larger FCTPLX stabilization than the free C_2H_4 system [Figure 4(*e*)]. These results suggest that the metal ion reduces the ESX destabilization but increases the FCTPLX stabilization, which seems important in the acceleration of the nucleophilic attack, as discussed later.

Electron Distribution.—The following features are found in the Mulliken population analysis (Figure 5): (1) As H_2O approaches C_2H_4, the electron population of the former gradually decreases, but both the electron populations of the C_2H_4 and metal gradually increase; (2) the attack of H_2O upon C_2H_4 increases the C^β atomic population but decreases that of C^α except in the final step ($R_{C^\alpha-O}$ = 1.8—1.4 Å) of the $[Li(C_2H_4)]^+$←OH_2 and $[HgH(C_2H_4)]^+$←OH_2 systems where the C^α atomic population slightly increases, perhaps due to the significant increase in the charge transfer from H_2O to C_2H_4, and simultaneously the C^β atomic population slightly decreases, probably because of the increase in charge transfer from C_2H_4 to metal.

The difference density maps were also analyzed according to the e.d.a. scheme, as shown in Figure 6. The map showing total difference density is almost the same as the sum of the difference

* Unfortunately, the ESX term of the $[HgH(C_2H_4)]^+$←OH_2 reaction system cannot be partitioned into ES and EX terms. The increase in the ESX destabilization could be, however, considered to result from the fact that the EX destabilization increases more than the ES stabilization, because both factors generally become large with decreasing distance between the two fragments.

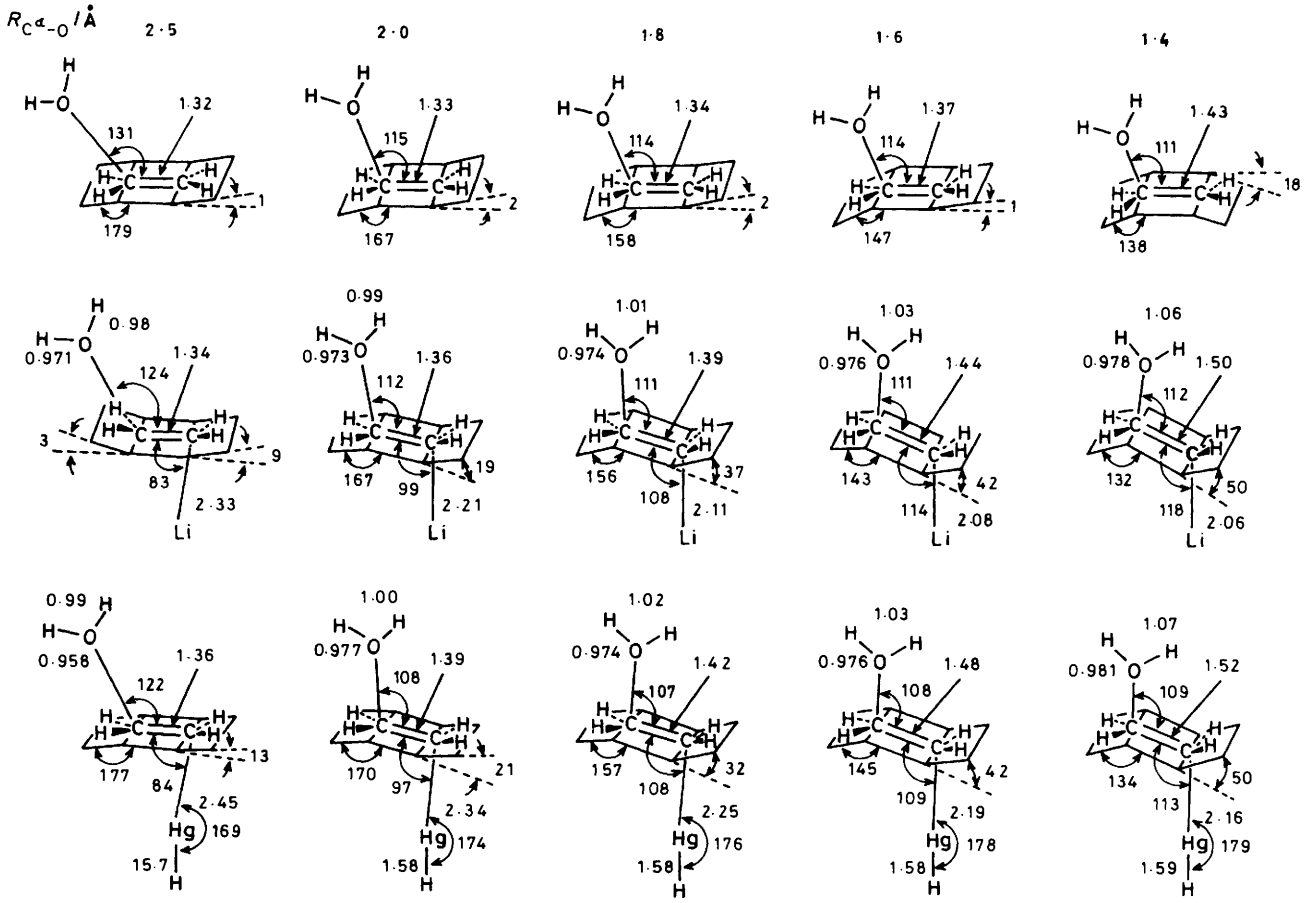

Figure 3. Optimized geometries of C_2H_4←OH_2, $[Li(C_2H_4)]^+$←OH_2, and $[HgH(C_2H_4)]^+$←OH_2. Distances in Å, angles in °. The bond distance O^1–H^1 (see Figure 1) is optimized in the presence of the second water molecule

densities of EX and FCTPLX, suggesting that the electron distribution is largely determined by these two interactions. In the EX difference density map, a considerable amount of electrons move from the C^{α} to the C^{β} atom. This feature is quite similar to the change in Mulliken population described above. In the difference density map of FCTPLX, a small but non-negligible amount of electrons is accumulated between H_2O and the C^{α} atom. Also, significant polarization is found in the metal–ethylene part, electron density decreasing near the C^{α} atom but increasing near C^{β}. In the $[Li(C_2H_4)]^+$←OH_2 system a small amount of electrons is accumulated near Li^+, suggesting charge transfer from C_2H_4 to Li^+. In the $[HgH(C_2H_4)]^+$←OH_2 system, electron density is decreased quite near to the mercury nucleus, perhaps due to the exchange repulsion between the *d*-electron cloud of Hg and the accumulated electron cloud of the C^{β} p_{π} orbital.* However, if the covalent radius of Hg is taken into consideration, electron density is increased in HgH^+, suggesting that electron transfer occurs from C_2H_4 to HgH^+. In conclusion, three kinds of electron flow, *i.e.* charge transfer from H_2O to C_2H_4, from C^{α} to C^{β}, and from C^{β} to metal, occur in the metal-accelerated nucleophilic attack, as shown in Scheme 2.

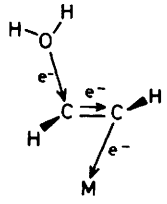

Scheme 2.

Important Orbital Mixing in Nucleophilic Attack.—Finally, we discuss why the above-mentioned changes in electron distribution and geometry are caused by the nucleophilic attack. The nucleophile offers the reaction system a donor orbital, which breaks the symmetry of the reaction system and induces several kinds of orbital mixing. Such orbital mixing is described approximately by the second-order perturbation (4)

$$\varphi_i = \varphi_i^0 + \sum_{m \neq i} \frac{H_{mi}}{\varepsilon_i^0 - \varepsilon_m^0} \cdot \varphi_m^0 + \sum_{m \neq i} \sum_{n \neq i} \left[\frac{H_{nm}H_{mi}}{(\varepsilon_i^0 - \varepsilon_m^0)(\varepsilon_i^0 - \varepsilon_n^0)} - \frac{H_{ii}H_{ni}}{(\varepsilon_i^0 - \varepsilon_n^0)^2} \right] \varphi_n^0 - \frac{1}{2} \sum_{m \neq i} \frac{H_{mi}H_{im}}{(\varepsilon_i^0 - \varepsilon_m^0)^2} \cdot \varphi_m^0 \quad (4)$$

where φ_i^0 represents a non-perturbed molecular orbital with energy ε_i^0 and H_{mn} is the resonance integral between the φ_m^0 and φ_n^0. In the C_2H_4←OH_2 system the π and π^* orbitals mix with the lone-pair orbital of the nucleophile, φ_l, and they are

* The electron accumulation on the C^{β} atom would result in large EX repulsion with the electron clouds of Hg which are mainly composed of 5*d* electrons, and would arise simultaneously to the charge transfer from C^{β} to HgH^+; this FCTPLX interaction reduces the Hg 5*d* orbital population but increases the Hg 6*s*,6*p* orbital population and the H atomic population.

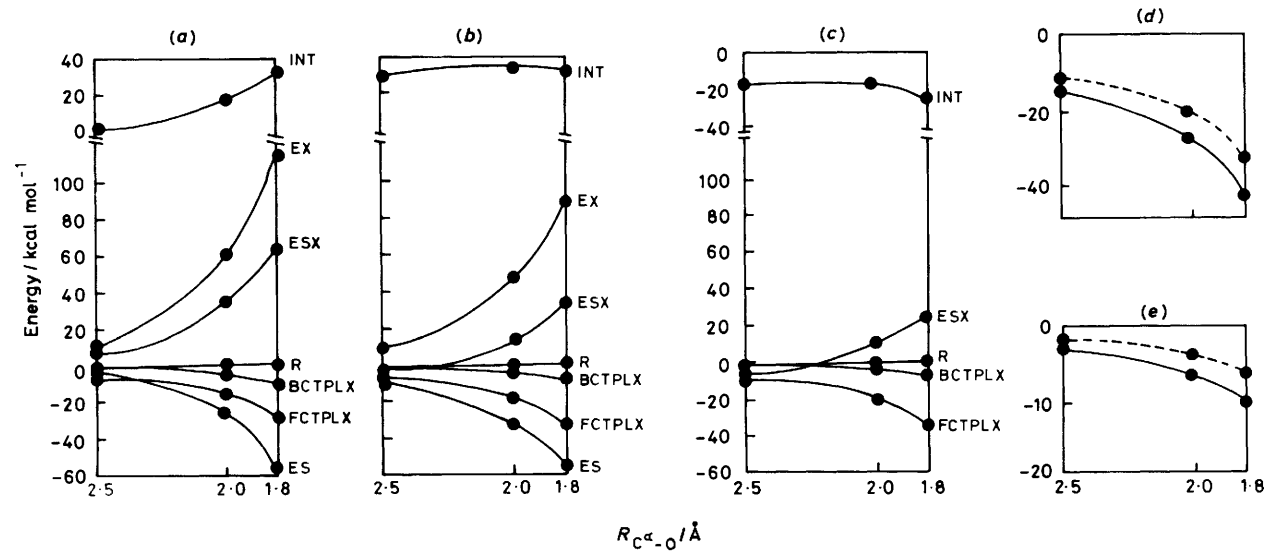

Figure 4. Energy components between $M(C_2H_4)$ and H_2O given as a function of $R_{C^{\alpha}-O}$. The 3 − 21 + G basis is used for the C atom. (*a*) C_2H_4←OH_2; (*b*) $[Li(C_2H_4)]^+$←OH_2; (*c*) $[HgH(C_2H_4)]^+$←OH_2; (*d*) ΔE_{ESX}; (*e*) ΔE_{FCTPLX}. $\Delta E_{ESX} = E_{ESX}[M(C_2H_4)\leftarrow OH_2] - E_{ESX}(C_2H_4\leftarrow OH_2)$, and $\Delta E_{FCTPLX} = E_{FCTPLX}[M(C_2H_4)\leftarrow OH_2] - E_{FCTPLX}(C_2H_4\leftarrow OH_2)$, where M = HgH^+ (——) or Li^+ (– – –)

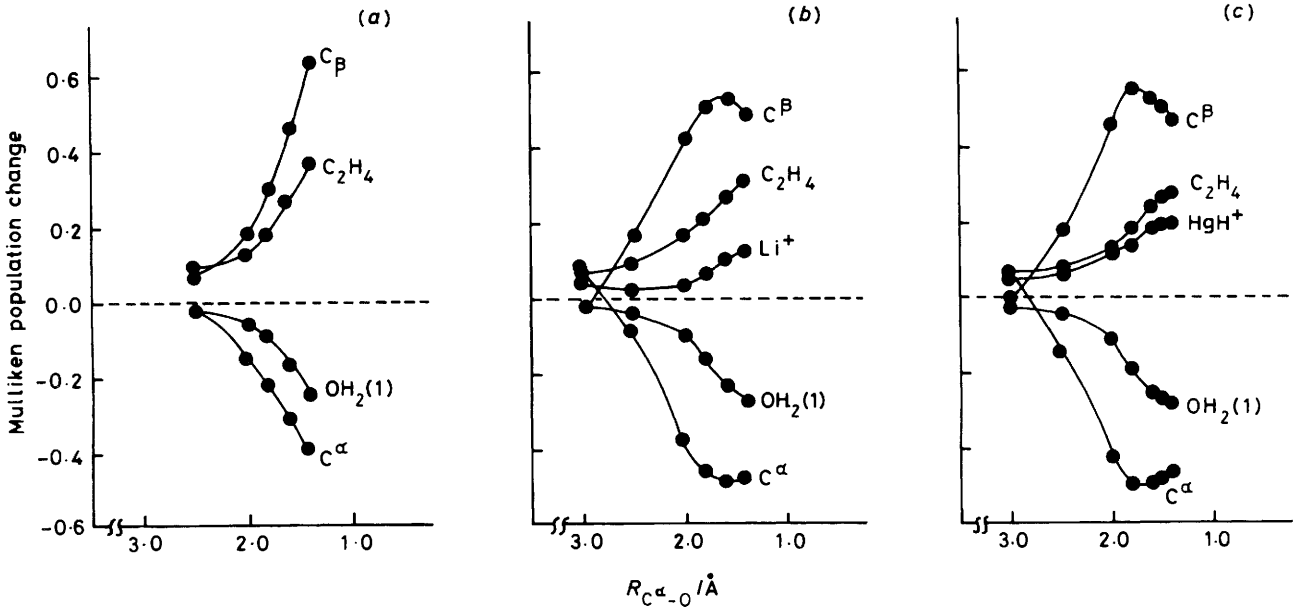

Figure 5. Mulliken population change caused by the approach of H_2O. The 3 − 21 + G basis is used for the C atom. Systems: (*a*) C_2H_4←OH_2; (*b*) $[Li(C_2H_4)]^+$←OH_2; (*c*) $[HgH(C_2H_4)]^+$←OH_2

reconstructed as new m.o.s, φ_1—φ_3, as shown in Figure 7[13] [Similar orbital mixing has been proposed in nucleophilic substitution at vinylic carbon (R. D. Bach and G. J. Wolber, *J. Am. Chem. Soc.*, 1984, **106**, 1401).] In these m.o.s the orbital mixing of the φ_2 orbital is considered to be the greatest, because of the smallest difference in orbital energies relating to the perturbation. The φ_2 orbital is composed mainly of the φ_{π} orbital, with which the φ_l orbital is mixed by way of anti-bonding, but the φ_{π^*} orbital is mixed by way of bonding with the φ_l orbital through the first and second mixing terms of equation (4), respectively. Such orbital mixing decreases the contribution of the C^{α} p_{π} orbital in φ_2, but increases that of the C^{β} p_{π} orbital, as shown in Figure 7.* These features are consistent with the contour map of total electron density and the Mulliken population analysis described above. The decrease in the C^{α} p_{π} orbital population induces electrostatic attraction between C^{α} and the nucleophile, and simultaneously reduces the exchange repulsion between the C^{α} p_{π} orbital and the nucleophile φ_l orbital. If a metal complex exists in the reaction

* The orbital mixing in the virtual φ_3 orbital increases the contribution of the C^{α} p_{π} orbital and reduces that of the C^{β} p_{π} orbital. Because the change found in the occupied level is opposite to that in the virtual space, the C^{α} p_{π} contribution must be decreased but the C^{β} p_{π} contribution increased by the nucleophilic attack in the occupied level, *i.e.* the mixing in the φ_2 orbital is larger than that in the φ_1 orbital (note that the mixing in φ_1 increases the C^{α} p_{π} population but decreases that of C^{β} p_{π}).

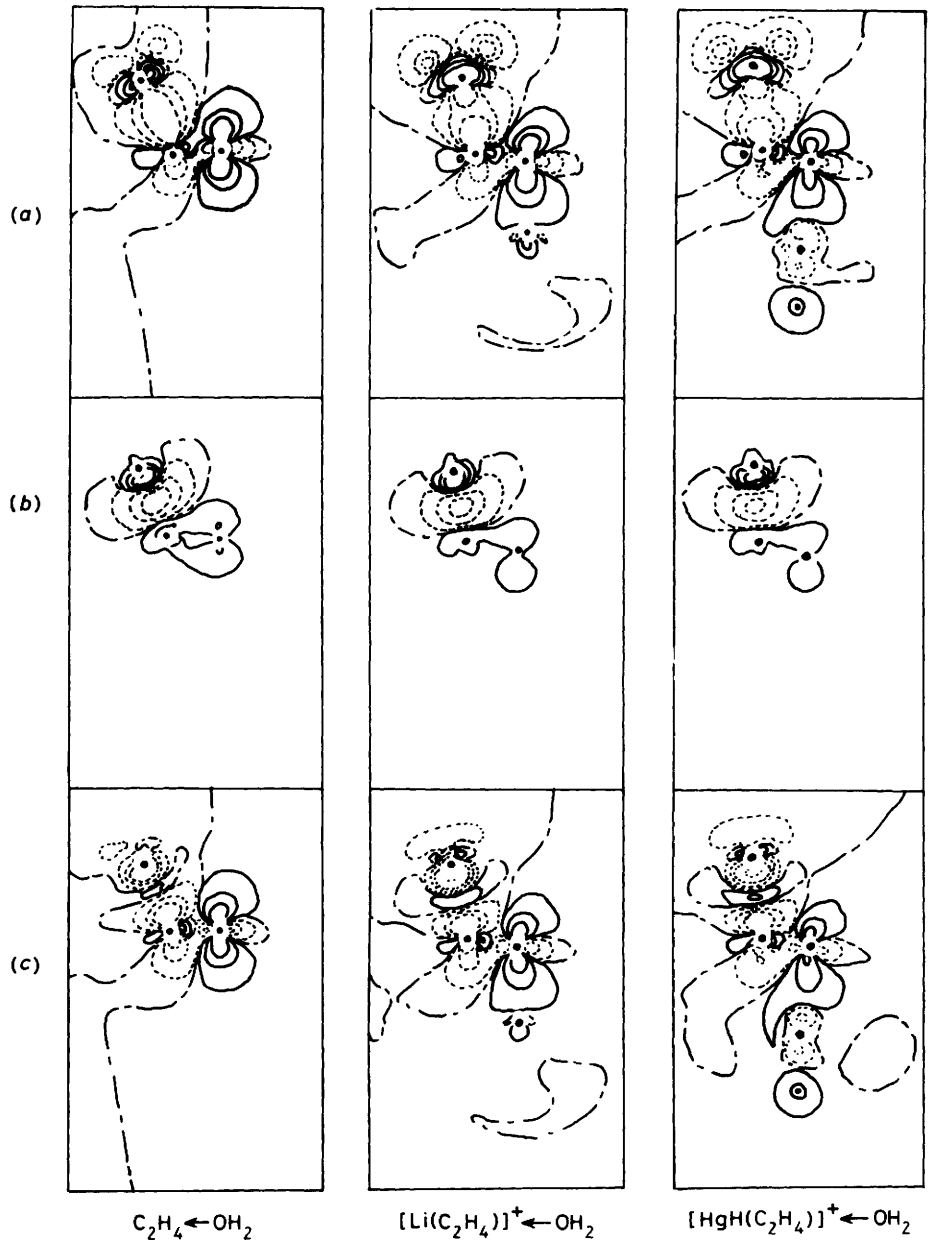

Figure 6. Difference density maps for the $M(C_2H_4)$←OH_2 system ($R_{C^\alpha-O}$ = 2.0 Å). The 3 − 21 + G basis is used for the C atom. ——, Increase in the electron density; – – –, decrease in the electron density; — – —, no change in the electron density. (*a*) Total difference density; (*b*) EX difference density; (*c*) FCTPLX difference density

system, the electrons accumulated on the C^β p_π orbital can be transferred to the metal through charge-transfer interaction and electrostatic attraction occurs between the positively charged metal and the negatively charged C^β atom. Thus, the metal ion would stabilize the reaction system, and the nucleophilic attack would be accelerated.

Let us examine the metal-accelerated nucleophilic attack in more detail. π-Back bonding is not considered to be significant in the C_2H_4 co-ordination because the *d* orbitals of Hg^{II} lie at low energies and Li^+ has no *d* orbital in its valence shell. Thus, four orbitals, φ_σ, φ_{σ^*}, φ_π, and φ_l, should be taken into consideration in the orbital mixing, as shown in Figure 8. Of the two occupied orbitals, φ_1 and φ_2, we need to examine φ_2 in detail because its orbital mixing is considered to be larger than that of φ_1 due to smaller difference in orbital energies. This orbital consists mainly of the φ_σ orbital, with which the φ_l, φ_{π^*}, and φ_{σ^*} mix as shown in Figure 8. (A detailed explanation is omitted here, because the present orbital mixing is essentially the same as that for C_2H_4←OH_2.) As a result, the C^α p_π orbital population decreases, that of C^β p_π increases, the Li–C^β bonding interaction becomes strong, but the Li–C^α weak, leading to opening of the $C^\alpha C^\beta$Li angle, lengthening of the Li–C^α distance, and shortening of the Li–C^β distance. Thus, the changes in geometry and electron distribution induced by the nucleophilic attack can be explained by the orbital mixing of φ_2.

It is interesting to examine why the mercury system accelerates the nucleophilic attack more than the lithium system does, when the $[HgH(C_2H_4)]^+$←OH_2 system includes essentially the same orbital mixing as $[Li(C_2H_4)]^+$←OH_2 does. The difference between the two systems becomes evident upon comparing the electronic structures of $[Li(C_2H_4)]^+$ and $[HgH(C_2H_4)]^+$. As shown by the Mulliken population in the

Table. Mulliken population analysis of $[Li(C_2H_4)]^+$ and $[HgH(C_2H_4)]^+$ using a 3-21 + G basis set

	C_2H_4	$[Li(C_2H_4)]^+$	$[HgH(C_2H_4)]^+$
M		2.210	11.492
s		2.111	1.311
p		0.099	0.288
d			9.893
C_2H_4	16.00	15.790	15.588

Table, the C_2H_4 ligand donates electrons to HgH^+ more readily than to Li^+. This means that HgH^+ has a greater ability to accept electrons than Li^+. The acceptor orbital of HgH^+ lies at -7.01 eV whereas the 2*s* orbital of Li^+ is at -5.29 eV. When the acceptor orbital becomes stable the φ_σ and φ_{σ^*} orbitals lie lower in energy, which increases the mixing of φ_{σ^*} with the φ_2 orbital. This mixing, including the bonding overlap between the C^α p_π and the nucleophile φ_l orbitals, decreases the C^α p_π contribution to φ_2, leading to a decrease in the exchange repulsion between the C^α p_π and the φ_l orbitals, as shown in Figure 8. Further, it increases the contribution of metal orbitals to φ_2, which means an increase in the charge transfer from C_2H_4 to HgH^+. Thus, the mercury system suffers only a small ESX destabilization and receives a large FCTPLX stabilization, by means of which the nucleophilic attack is accelerated.

In conclusion, the metal complex greatly accelerates nucleophilic attack on a complexed olefin when the acceptor orbital of the metal lies low in energy, as in the mercury(II) complex. Thus, the energy level of the metal acceptor orbital is an important factor in the metal-accelerated nucleophilic attack. Changes in electronic structure and geometry caused by the nucleophilic attack can clearly be understood in terms of the mixing between the φ_σ, φ_{π^*}, and φ_{σ^*} orbitals of $M(C_2H_4)$ and the φ_l orbital of the nucleophile.

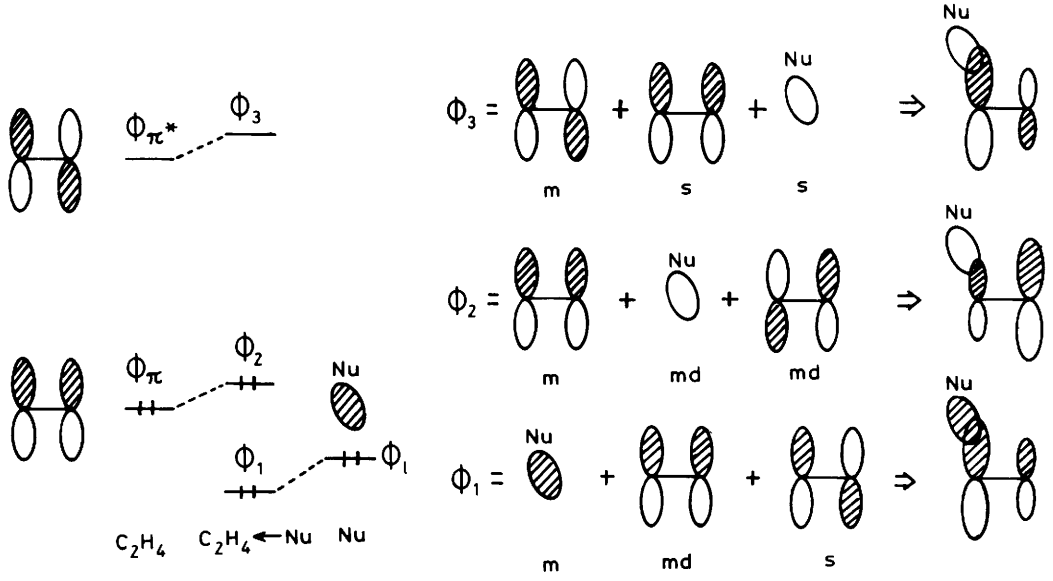

Figure 7. Schematic picture of orbital mixing in the C_2H_4←OH_2 system. Nu = Nucleophile; m = main, md = medium, and s = small

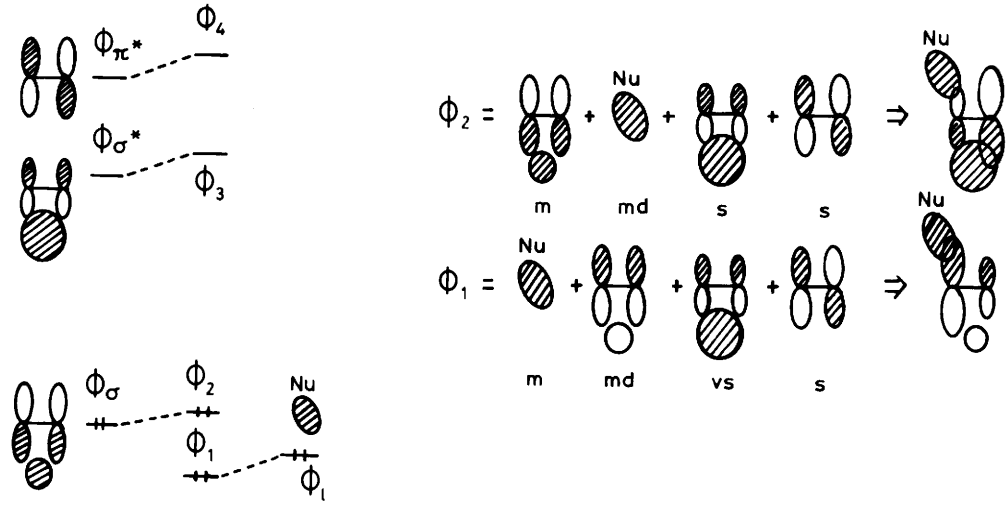

Figure 8. Schematic picture of orbital mixing in the $M(C_2H_4)$←OH_2 system (M = Li^+ or HgH^+). vs = Very small

Acknowledgements

The authors are grateful to Professor K. Morokuma for his kind support of this work. All of the calculations were carried out with a Hitac-200H at the computer centre of the Institute for Molecular Science.

References

1 G. Henrici-Olive and S. Olive, 'Coordination and Catalysis,' Verlag Chemie, Weinheim, 1977; G. Wilkinson (ed.), 'Comprehensive Organometallic Chemistry. The Synthesis Reactions and Structures of Organometallic Compounds,' Pergamon Press, Oxford, 1982; B. M. Trost, *Tetrahedron*, 1977, **33**, 3615.
2 S. Sakaki, H. Kato, H. Kanai, and K. Tarama, *Bull. Chem. Soc. Jpn.*, 1974, **47**, 377; B. Akermark, M. Almemark, J. Almlöf, J-E. Bäckvell, B. Roos, and A. Stogard, *J. Am. Chem. Soc.*, 1977, **99**, 4617; S. G. Davies, M. L. H. Green, and D. M. P. Mingos, *Tetrahedron*, 1978, **34**, 3047; J-E. Bäckvall, E. E. Björkman, L. Pettersson, and P. Siegbahn, *J. Am. Chem. Soc.*, 1984, **106**, 4369.
3 O. Eisenstein and R. Hoffmann, *J. Am. Chem. Soc.*, 1980, **102**, 6148; 1981, **103**, 4308.
4 F. Freeman, *Chem. Rev.*, 1975, **75**, 439.
5 K. Morokuma, S. Kato, K. Kitaura, I. Ohmine, S. Sakai, and S. Obara, Institute for Molecular Science, Computer Center Library program 0372, 1980.
6 H. Basch and S. Topiol, *J. Chem. Phys.*, 1979, **71**, 802.
7 J. S. Binkley, J. A. Pople, and W. J. Hehre, *J. Am. Chem. Soc.*, 1980, **102**, 939.
8 C. Clark, J. Chandraseknar, G. W. Spitznagel, and P. R. Schleyer, *J. Comput. Chem.*, 1983, **4**, 294.
9 P. Pulay, 'Modern Theoretical Chemistry,' ed. H. F. Schaeffer, III, Plenum, New York, 1977, p. 153.
10 K. Kitaura, S. Obara, and K. Morokuma, *Chem. Phys. Lett.*, 1981, **7**, 452.
11 W. Lau, J. C. Hoffmann, and J. K. Kochi, *J. Am. Chem. Soc.*, 1982, **104**, 5515.
12 K. Morokuma, *J. Chem. Phys.*, 1971, **55**, 1236; *Acc. Chem. Res.*, 1977, **10**, 325; K. Kitaura and K. Morokuma, *Int. J. Quantum Chem.*, 1976, **10**, 325; K. Kitaura, S. Sakaki, and K. Morokuma, *Inorg. Chem.*, 1981, **20**, 2292.
13 S. Inagaki and K. Fukui, *Chem. Lett.*, 1974, 509; S. Inagaki, H. Fujimoto, and K. Fukui, *J. Am. Chem. Soc.*, 1976, **98**, 4054.

Received 4*th March* 1986; *Paper* 6/438